Accelerometer-Based Gait Recognition by Sparse Representation of Signature Points With Clusters

Yuting Zhang, Gang Pan, Kui Jia, Minlong Lu, Yueming Wang, and Zhaohui Wu

***Abstract*—Gait, as a promising biometric for recognizing human identities, can be nonintrusively captured as a series of acceleration signals using wearable or portable smart devices. It can be used for access control. Most existing methods on accelerometer-based gait recognition require explicit step-cycle detection, suffering from cycle detection failures and intercycle phase misalignment. We propose a novel algorithm that avoids both the above two problems. It makes use of a type of salient points termed signature points (SPs), and has three components: 1) a multiscale SP extraction method, including the localization and SP descriptors; 2) a sparse representation scheme for encoding newly emerged SPs with known ones in terms of their descriptors, where the phase propinquity of the SPs in a cluster is leveraged to ensure the physical meaningfulness of the codes; and 3) a classifier for the sparse-code collections associated with the SPs of a series. Experimental results on our publicly available dataset of 175 subjects showed that our algorithm outperformed existing methods, even if the step cycles were perfectly detected for them. When the accelerometers at five different body locations were used together, it achieved the rank-1 accuracy of 95.8% for identification, and the equal error rate of 2.2% for verification.**

***Index Terms*—Accelerometers, biometrics, gait dataset, gait recognition, signature points (SPs), sparse representation.**

I. Introduction

In RECENT years, the portable and wearable devices with smartness have greatly interested the industrial worlds. Manufacturers have incorporated additional computing capacity and various sensors (e.g., GPS [1] and accelerometers) into cellphones, watches, shoes, clothes, and other portable/wearable items, which makes a world of pervasive computing possible [2].

With built-in accelerometers, these items can be aware of the body motion of users, which inspired the academic interest in using the motion characters of human body for various tasks, including clinical condition monitoring [3], action/gesture categorization [4]–[6], and identity recognition. In particular, accelerometer-based identity recognition using body motion is promising in preventing the misuse of smart devices and the systems linked with them.

Since walking is a daily activity, human gait can be measured in daily life without explicitly asking the subjects to walk. This fact distinguishes gait from other accelerometer-measurable actions, like gestures, as well as other commonly used biometrics, such as fingerprints, signatures, and face photos, whose acquisition usually interrupts the subjects from normal activities for explicit participation.

The intrusiveness of measuring gait makes gait favorable for user-friendly identity recognition. In particular, as portable or wearable accelerometers can monitor gait continuously at arbitrary time, accelerometer-based gait recognition would be especially well in continuous identity reverification [7], which may help secure the access to sensitive carry-on items like cellphones and car keys (provided they are smart).

It is true that gait can be monitored through media other than accelerometers, e.g., distant camera, gyroscopes [8], [9], foot pressure sensors [10], [11], and step sound recorders [12]. Among gait recognition methods relying on various media, those based on camera vision were intensively researched [13]–[18] in the past decade.

Compared with camera-based and other nonaccelerometer-based gait measurements, acceleration can reflect the dynamics of gait more directly and faithfully. Indeed, accelerometer-based gait recognition do not suffer from the long-term existing problems for vision-based methods, like occlusions, clutter, 3-D viewpoint changes, illumination variations, and appearance alternations, as well as other perceptual distortions.

Most existing methods for accelerometer-based gait recognition detect step cycles, and correspond acceleration signals in different cycles, usually by linear warping. This paradigm has two main drawbacks: 1) cycle detection methods are usually error-prone, making the recognition methods fragile to occasional abnormalities like temporary walking pauses and 2) most methods ignore the intercycle phase misalignment, which in fact widely exists in gait acceleration data.

To remedy the intercycle phase misalignment problem, some methods explicitly align the step cycles by dynamic time warping (DTW) [19], [20]. However, their performance is limited by their dependency on cycle detection and the instability of unconstrained DTW. Alternatively, Pan *et al.* [21] extracted a particular kind of salient points termed signature

Manuscript received November 25, 2013; revised August 19, 2014; accepted September 16, 2014. Date of publication November 20, 2014; date of current version August 14, 2015. This work was supported in part by the National Key Basic Research Program of China under Grant 2013CB329504 and in part by the Program for New Century Excellent Talents in University under Grant NCET-13-0521. This paper was recommended by Associate Editor B. W. Schuller. *(Corresponding author: G. Pan.)*

Y. Zhang, G. Pan, M. Lu, and Z. Wu are with the Department of Computer Science, Zhejiang University, Hangzhou 310027, China (e-mail: zyt@zju.edu.cn; gpan@zju.edu.cn; ymlml@zju.edu.cn; wzh@zju.edu.cn).

K. Jia is with the Department of Electrical and Computer Engineering, Faculty of Science and Technology, University of Macau, Macau, China (e-mail: kuijia@gmail.com).

Y. Wang is with the Qiushi Academy for Advanced Studies, Zhejiang University, Hangzhou 310027, China (e-mail: ymingwang@gmail.com).

Color versions of one or more of the figures in this paper are available online at http://ieeexplore.ieee.org.

Digital Object Identifier 10.1109/TCYB.2014.2361287

points (SPs) on gait acceleration series, and avoided the intercycle misalignment problem by SP matching. While setting forth a promising direction, Pan *et al.*'s method [21] still requires cycle detection, as it uses the relative location within step cycle for constraining the matching problem.

In this paper, we propose a novel accelerometer-based gait recognition method, which avoids cycle detection and the intercycle misalignment problem. In particular, we improve the existing algorithm of SP localization and descriptors [21] by a multiscale extension, and represent a gait acceleration series by a rich collection of SPs. We cluster the SPs from all the gallery series according to the similarity of their descriptors, and illustrate the phase propinquity of the SPs within a cluster. Given a probe gait acceleration series, we encode every of its SPs, in terms of the SP descriptor, as a sparse linear combination of the SPs from all the gallery series. In this step, we constrain the code to concentrate only in the gallery cluster(s) that is/are most similar to the descriptor of the SP to be encoded. We will demonstrate later that this constraint can implicitly force an SP to be encoded with those whose phases are close to it, which makes the obtained code physically meaningful. After that, we recognize the probe series by a novel classifier for sparse-code collection (CSCC), where we incorporate the subject-wise reconstruction errors of each SP into a probabilistic framework, and formulate CSCC as a problem of maximum a posteriori (MAP) estimation. Finally, we generalize our method for multiple accelerometers.

We built a dataset called ZJU-GaitAcc, which, to the best of our knowledge, is the first publicly available dataset of gait acceleration series for identity recognition. Experimental results on ZJU-GaitAcc demonstrated that the proposed method outperformed existing methods and achieved significant performance increase with more accelerometers.

We summarize the main contributions of this paper.

1) We develop the multiscale SP extraction method, and obtain a rich and stable feature collection representation of gait acceleration series.
2) We designed a sparse coding scheme to obtain physically meaningful sparse representation of SPs.
3) We propose CSCC to recognize gait acceleration series represented by SP collections. It avoids cycle detection, and is ready for the multiaccelerometer scenario.
4) We publish the ZJU-GaitAcc dataset, which covers 175 subjects and five body locations.

In the rest of this paper, we review previous work (Section II), develop the SP extraction method together with showing the phase propinquity related to SP clusters (Section III), present the SP encoding scheme, and CSCC (Section IV), describe the ZJU-GaitAcc dataset (Section V), and report experimental results (Section VI).

II. Previous Work

Gait recognition using accelerometers is a newly emerged topic. It was first touched by Morris [36] and then formally addressed by Mäntyjärvi *et al.* [22]. Now, more and more pieces of work have focused on this topic. Some early methods processed data in the frequency domain [22], [26], [31] or used the histograms of entire acceleration series [22], [24], [25], [27]. Later, they were largely surpassed by methods making direct use of original series in the time domain.

According to the ways for handling step cycles, we categorize most existing time-domain methods into three types: 1) cycle comparison based on length normalization; 2) cycle comparison by alignment; and 3) methods without cycle comparison. They are summarized in Table I, and reviewed in the following.

A. Cycle Comparison by Length Normalization

Mäntyjärvi *et al.* [22] and Ailisto *et al.* [23] measured the similarity between two gait acceleration series recorded at waists by the linear correlation between the averaged step cycles of the two series. To obtain the average step cycle of a series, all the step cycles are detected and normalized to the same length (dimensions). Vildjiounaite *et al.* [26] used a similar method for recognizing gait acceleration series collected at hands, breast pockets, or hip pockets. In these algorithms, the cycle detection methods cannot distinguish the left and the right steps, so two averaged half (left/right) cycles with an odd/even parity are computed for a series. This character is referred to as "avg. step" in Table I.

The above methods induced a widely used algorithm framework based on normalizing the length of step cycles: 1) detecting step cycles; 2) normalizing the length of each cycle so that all the cycles have the identical number of samples; 3) constructing cycle templates for gait acceleration series; and 4) recognizing gait by cycle template comparisons.

Gafurov *et al.* [24], [25], [27] followed this framework, and averaged full cycles (a left and a right step) in a series to be the cycle template, which we refer to as "avg. cycle" in Table I. They recorded gait acceleration at waists or ankles, and investigated different averaging methods and metrics for template comparisons. Gafurov *et al.* [37], [38] also studied the robustness of their algorithms against impersonation attacks.

Recently, more sophisticated methods were proposed for cycle comparison based on length normalization. Inspired by the famous "eigenface" method [39] for face recognition, Bours and Shrestha [28] used eigenstep representation to improve the recognition accuracy. Cycle template similarity is computed in the low-dimensional subspace obtained by principle component analysis (PCA). Gafurov *et al.* [29] compared all the step cycles between two series (referred to as "cycle matching") instead of using the average cycles. Juefei–Xu *et al.* [30] took the intercycle variance as the cycle template.

In the aforementioned methods, the cycle-length normalization is done by linear interpolation, which appears to be effective as Juefei–Xu *et al.* [30] argued. However, as previously discussed in Section I, the intercycle misalignment cannot be sufficiently corrected by linear interpolation.

B. Cycle Comparison by Alignment

To solve the intercycle misalignment problem, Liu *et al.* [19], [31], and Derawi *et al.* [20] used DTW to explicitly align the acceleration in different step cycles. Derawi *et al.* [32] made further improvement by integrating

TABLE I
SOME RELATED WORK ON ACCELEROMETER-BASED GAIT RECOGNITION METHODS

Method Type	Year	Studies	Locations	RR	EER	#Subj.	Characteristics
Cycle comparison based on length normalization	2005	Mäntyjärivi et al. [22]	Waist	/	7.0%	36	Avg. step, corr.
	2005	Ailisto et al. [23]	Waist	/	6.4%	36	Avg. step, corr.
	2006	Gafurov et al. [24], [25]	Waist	/	9%	21	Avg. cycle, p-value in t-test
	2006	Vildjiounaite et al. [26]	Hand	/	17.2%	31	Avg. step, corr.
			Breast pocket	/	14.8%	31	
			Hip pocket	/	14.1%	31	
	2007	Gafurov et al. [27]	Trouser pocket	86.3%	7.3%	50	Avg. cycle, L1 dist.
	2010	Bours et al. [28]	Left hip	/	1.6%	60	Eigenstep (PCA)
	2010	Gafurov et al. [29]	Ankle	/	[a]16.4%	30	Cycle matching
	2012	Juefei-Xu et al. [30]	Right pocket	/	3.6%	36	Variance as feature
Cycle comparison by alignment	2007	Liu et al. [19]	Waist	/	6.7%	35	DTW
	2007	Liu et al. [31]	Waist	/	5.6%	21	DTW, avg. cycle
	2010	Derawi et al. [20]	Trouser pocket	/	20.1%	51	DTW, avg. cycle
	2010	Derawi et al. [32]	Left leg	/	5.7%	60	Cycle matching, DTW, CRM
	2011	Trung et al. [33]	Back bag	/	6.0%	32	Self-DTW, cycle matching, CRM
	2012	Trung et al. [34]	Waist	/	[b]10%	736	the same as above
Methods without cycle comparison	2009	Pan et al. [21]	Wrist, upper arm, hip, knee, ankle	96.7%	/	30	SP, NN, voting scheme
	2012	Nickel et al. [35]	Trouser pocket	/	[c]10.3%	48	HMM
	2013	This paper	Wrist, upper arm, hip, knee, ankle	95.8%	2.2%	175	SP, sparse coding, CSCC

Remarks: RR – recognition rate (or, rank-1 accuracy, for identification); EER – equal error rate (for verification); #Subj – the number of subjects. a. a typical result in [29]; b. approximated from the ROC curve reported in [34]; c. approximated from the reported FNR (10.42%) and FPR (10.29%).

cyclic rotation metric (CRM) and cycle matching scheme. One drawback of these methods is that DTW might warp the series too much so that the series loses its discriminative patterns. To register the gallery step cycles in a more stable way, Trung *et al.* [33] used self-DTW [40] to assign every sample in a series with an aligned phase, and presented a regularization method to reduce unwanted warping. Unfortunately, as they used DTW for step-cycle comparison in the test stage, the only contribution of the gallery registration seems to be cycle detection. After all, alignment/warping does not affect the DTW distance.

C. Methods Without Cycle Comparison

Pan *et al.*'s method [21] avoided explicit phase registration. It extracted SPs on acceleration series, labeled the SPs on a probe series, and predicted its identity by the SP labels. In particular, they labeled SPs by the nearest neighbor (NN) classifier constrained by the propinquity of SPs unregistered phases.

One common bottleneck for cycle-comparison methods and Pan *et al.*'s method [21] is the dependence on cycle detection. Although endeavors have been made to improve the robustness of cycle detection techniques [32], [41], they might still fail in some cases. Nickel *et al.* [35] performed HMM on signal segments with a fixed length, which did not need cycle detection. However, this method ignored the misalignment among segments. Fortunately, our algorithm proposed in this paper both stays away from cycle detection and avoids the problem of intercycle misalignment.

III. SPs: FEATURE COLLECTIONS OF GAIT ACCELERATION SERIES

Gait is the motion of a walking body, whose dynamics can be faithfully reflected by the acceleration of body sections. We measure it at specific body locations by wearable accelerometers with three orthogonal sensing directions. The obtained acceleration can be featured with its magnitude, one of its x, y, z components, the included angle between two components, etc. To get the invariance against the orientation changes of accelerometers, we use the acceleration magnitude, and the acceleration measured a one body location constitute a scalar time series.

Let $a(t) \in \mathbb{R}$ be the function representing a gait acceleration series. We localize SPs at informative localities of $a(t)$s scale-space, attach them with local descriptors, and represent $a(t)$ as a collection of SPs. Unlike Pan *et al.* [21], we do not limit SPs in a single scale, so the SPs would be richer in quantity and robust to minor walking speed variations.

A. SP Extraction—Localization and Descriptors

Like Pan *et al.* [21], we localize the SPs of $a(t)$ at the extrema of $a(t)$s difference of Gaussian (DoG) pyramid.

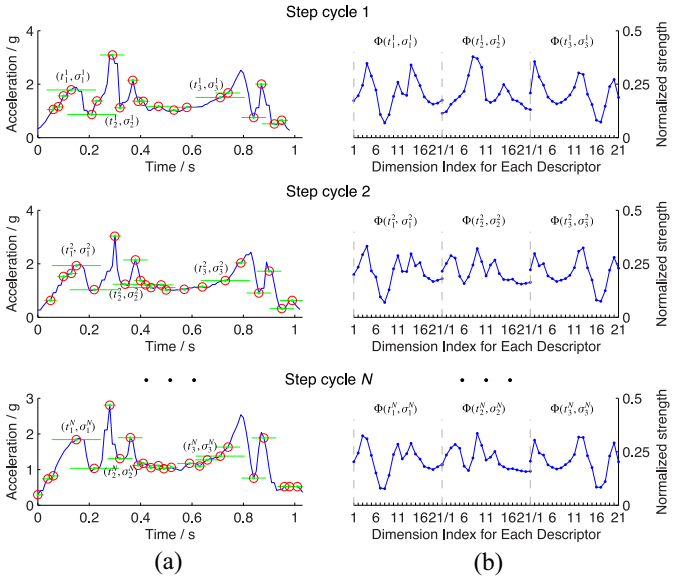

Fig. 1. SPs extracted from different step cycles in a gait acceleration series of one subject recorded at the right ankle. (a) Green dots with red circles indicate the locations of SPs. The green horizontal lines attached with them suggest the scales of SPs. In each step cycle, three SPs are marked with notations. For $i = 1, 2, 3$, the SPs (t_i^1, σ_i^1), (t_i^2, σ_i^2), $\ldots$, (t_i^N, σ_i^N) are corresponded because they are at the same cycle phase in different step cycles. (b) Descriptors of the marked SPs are shown. The corresponding SPs in different step cycles have similar descriptors.

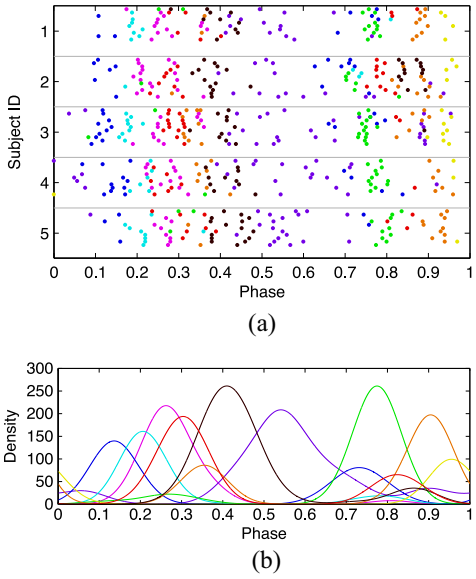

Fig. 2. SPs in clusters. SPs were extracted from the gait acceleration series of 20 subjects recorded at right ankles, and were grouped into nine clusters, where each cluster associates with a distinct color. (a) Scatters of cyclical locations (first five subjects). (b) PDFs of SP phases generated by kernel density estimator.

These extrema are shown to be stable, scale-invariant, and at informative localities [42].

Let us write $G_\sigma(t)$ for the zero-mean Gaussian function with variance σ^2, say

$$G_\sigma(t) = \frac{1}{\sqrt{2\pi}\sigma} \exp\left(-\frac{t^2}{2\sigma^2}\right). \tag{1}$$

The DoG function can be written as

$$D_\sigma^\gamma(t) = G_{\gamma\sigma}(t) - G_\sigma(t) \tag{2}$$

where $\gamma > 1$ (here simply, $= 2$) is the multiplicative factor. The DoG responses of $a(t)$ is then denoted by

$$b(t, \sigma) = \left(a * D_\sigma^\gamma\right)(t) \tag{3}$$

where "$*$" denotes convolution, and γ is constant. We localize the SPs of $a(t)$ at the extrema of $b(t, \sigma)$. In practice, we also consider the natural blur of the series a,[1] and replace D_σ^γ with $D_{\sigma-\sigma_N}^\gamma$ in (3), where σ_N is the scale for the natural blur.

Instead of continuously searching $b(t, \sigma)$, we find extrema in an τ-layer pyramid of discrete series

$$b[t, i] = b\left(t, \gamma^{i-1}\sigma_0\right) \quad \text{for } i = 1, 2, \ldots, \tau \tag{4}$$

where t is the discrete time stamp, i is the layer index, and σ_0 is the base scale. We can efficiently compute $b[t, i]$ as the difference of the Gaussian pyramid with scales $\{\gamma^i\sigma_0\}_{i=0}^\tau$. Any point that is simultaneously greater or smaller than its eight neighbors is taken as an extremum of $b[t, i]$. Let (t, i) be an extremum of $b[t, i]$. We locate the corresponding SP in $b(t, \sigma)$ at $(t, \gamma^{i-1}\sigma_0)$. To improve the stability of SP localization, we will reject the above SP if $|b[t, i]|$ is too small. Fig. 1(a) gives an illustration of SPs.

The time-domain neighborhoods of SPs have locally high contrast. We define the descriptor of an SP at (t, σ) by its neighborhood in the time domain as

$$\Theta(t, \sigma) = \frac{(\theta_1, \theta_2, \ldots, \theta_h)^T}{\|(\theta_1, \theta_2, \ldots, \theta_h)\|_2} \in \mathbb{R}^h \tag{5}$$
$$\text{where } \theta_i = (a * G_\sigma)\left(t + \left(i - \tfrac{h+1}{2}\right)\sigma\varepsilon\right).$$

It uniformly samples h points around t from the σ-scale of $a(t)$, i.e., $a(t)$s response to $G_\sigma(t)$, with the scale-dependent interval $\sigma\varepsilon$, and normalizes the obtained vector to unit length. The SP descriptor has invariance to both scale and amplitude changes, which would together contribute to its robustness against walking speed variations. In Fig. 1(b), we show some SP descriptors. Now, we represent a gait acceleration series by the extracted SP collection.

B. Phase Propinquity of SPs in Cluster

SPs can be grouped into clusters according to the similarity of their descriptors, where each cluster associates with a type of similar acceleration patterns. As it is shown in Fig. 2(a), the SPs in a cluster are usually close to each other in terms of their cycle phase. We term this property as phase propinquity. Fig. 2(b) shows the estimated probability distribution function (PDF) of the phases of the SPs in different clusters. Except for some subsidiary peaks, the distribution for one cluster mainly concentrates in a small phase interval, which gives more evidence for the phase propinquity. Although the phases are not registered between cycles, the phase propinquity still indicates that the majority of the SPs in a cluster describe the same stage of gait motion.

[1]Due to the precision limitation of the sensor, the series are often blurred by nature. We use a Gaussian filter with a small variance to model this effect.

The phase propinquity is intuitive for the SPs of the same subject. For one subject, the gait patterns are generally consistent among different step cycles. The acceleration patterns at nearby step-cycle phases are similar, and those in distant phases are likely be different [Fig. 1(a)]. As the SP descriptors are actually temporal context around SPs, the SPs located at close step-cycle phases are likely to be grouped into the same cluster [Fig. 1(b)], and those at distant phases into different clusters. Inversely, SPs in the same cluster can show phase propinquity with a high chance.

For different subjects, on the one hand, their gait patterns still have much similarity. After all, human gait is a particular type of movement that holds a common pattern. Consequently, SPs at nearby step-cycle phases still tends to be clustered together, so the phase propinquity can hold across different subjects. On the other hand, as to recognition, finding the correct correspondence among the SPs of the same subject is much more important than doing it for different subjects. Even if the phase propinquity across subjects may not as stable as that for the same subject, it will not matter much for the recognition algorithm we are going to present.

IV. SP Sparse Representation and SP-Collection Recognition

In this section, we present our method for recognizing gait acceleration series using their SP collections. In particular, we encode individual SPs in terms of their descriptors by sparse representations with implicitly consideration of their phase. We then recognize a gait acceleration series by probabilistically fusing the errors for subject-wisely reconstructing its SPs from their sparse code.

Suppose that the gallery contains gait acceleration series of q known subjects. For the ith subject's gallery series, let n_i denote the total SP number, $\mathbf{x}_j^{\langle i\rangle} \in \mathbb{R}^h$ denote jth SP in terms of its descriptor,[2] and $\mathbf{X}_i = [\mathbf{x}_1^{\langle i\rangle}, \mathbf{x}_2^{\langle i\rangle}, \ldots, \mathbf{x}_{n_i}^{\langle i\rangle}] \in \mathbb{R}^{h\times n_i}$. We further concatenate $\{\mathbf{X}_i\}_{i=1}^q$ into a larger matrix $\mathbf{X} = [\mathbf{X}_1, \mathbf{X}_2, \ldots, \mathbf{X}_q] \in \mathbb{R}^{h\times n}$, where $n = \sum_{i=1}^q n_i$.

Given a probe series with unknown identity, let us write $\mathcal{Y} \subset \mathbb{R}^h$ for its SP collections in terms of SP descriptors. To recognize this series, we first encode each SP in $\mathcal{Y}$ with the dictionary $\mathbf{X}$, and then propose CSCC for both identification and verification purpose.

A. Sparse Representation of SPs With Clusters in Dictionary

For an SP $\mathbf{y} \in \mathcal{Y}$, we intend to encode it as a linear combination with the columns of $\mathbf{X}$. Without additional constraint, $\mathbf{y}$ may be encoded with SPs extracted at any step-cycle phase, which may mess up localities for different stages of gait motion (e.g., the initial contact, loading response, mid stance, etc. [43]) and make $\mathbf{y}$s code physically meaningless.

At first glance, in order to encode $\mathbf{y}$ with SPs extracted at nearby phases, we need compute all the SPs phases based on step-cycle detection or accurate phase registration, which we try to avoid in our method. Fortunately, this goal can also be roughly achieved by leveraging the phase propinquity of SPs clustered in terms of descriptor similarity (Section III-B). In particular, we group the columns of $\mathbf{X}$ into r clusters[3] by the k-means algorithm, find the sub-dictionary composed of the u clusters most similar to $\mathbf{y}$, and constrain $\mathbf{y}$s code to concentrate only in this sub-dictionary. According to the discussion in Section III-B, most SPs in the chosen sub-dictionary would be extracted at phases close to $\mathbf{y}$s.

Let $c_j \in \{1, 2, \ldots, r\}$, $1 \le j \le n$ denote the cluster label of the jth column of $\mathbf{X}$, $\mathbf{w}_k \in \mathbb{R}^h$ denote the center (Euclidean mean) of the kth groups, and $\mathbf{W} = [\mathbf{w}_1, \mathbf{w}_2, \ldots, \mathbf{w}_r] \in \mathbb{R}^{h\times r}$. We compute the distance between $\mathbf{y}$ and $\mathbf{w}_k$ $(k = 1, 2, \ldots, r)$ as

$$d_k = \min_{\alpha} \|\mathbf{y} - \alpha\mathbf{w}_k\|_2$$

where $\alpha > 0$ is used for rescaling the cluster center. Sorting $\{d_k\}_{k=1}^r$ in ascending order, we get $d_{k_1}, d_{k_2}, \ldots, d_{k_r}$. The index set of the clusters in the chosen sub-dictionary is $\mathcal{K} = \{k_1, k_2, \ldots, k_u\}$.

Now, we will encode $\mathbf{y}$ as a linear combination of the elements in the chosen sub-dictionary. By introducing the ℓ^0-norm constraint, we can make $\mathbf{y}$s code concentrate only in a few most relevant elements in the sub-dictionary, which may benefit the discriminativeness of $\mathbf{y}$s code. More specifically, $\mathbf{y}$s code is obtained by solving

$$\boldsymbol{\beta}^* = \arg\min_{\boldsymbol{\beta}} \|\mathbf{y} - \boldsymbol{\beta}\mathbf{X}\|_2 \tag{6}$$

$$\text{s.t. } \|\boldsymbol{\beta}\|_0 \le v, \text{ and } \beta_j = 0 \text{ if } c_j \notin \mathcal{K} \tag{7}$$

where the ℓ^0-norm $\|\boldsymbol{\beta}\|_0$ is the number of nonzero entries in $\boldsymbol{\beta}$, $v \in \mathbb{N}^+$ constrains the maximum number of nonzero entries in $\mathbf{y}$s code, and the second part of (7) constrains the encoding to be conducted with the sub-dictionary. A reasonable local solution to (6) can be obtained by the orthogonal matching pursuit (OMP) [44]–[46] algorithm. Thanks to pruning the whole dictionary to a subset, the problem scale of (6) is not large, which enables OMP to produce a convenient solution.

B. Recognition by CSCCs

With the SP collection $\mathcal{Y}$ of the probe, we will formulate the recognition task as a probabilistic decision problem. Let us write l for the random variable indicating the identity of the probe series. For an SP $\mathbf{y} \in \mathcal{Y}$, we will define $p(l = i|\mathbf{y})$ based on its sparse representation; and taking the elements of $\mathcal{Y}$ as independent observations, we will obtain $p(l = i|\mathcal{Y})$.

Let us write $\boldsymbol{\beta}^*$ for the sparse code of $\mathbf{y} \in \mathcal{Y}$, and let $\mathbf{X}_{(i)} = \left[\mathbf{O}_1, \ldots, \mathbf{O}_{i-1}, \mathbf{X}_i, \mathbf{O}_{i+1}, \ldots, \mathbf{O}_q\right]$ for $i = 1, 2, \ldots, q$, where $\mathbf{O}_i$ is the $h \times n_i$ zero matrix. Note that only the sub-matrix of $\mathbf{X}$ associating with the ith subject is kept in $\mathbf{X}_{(i)}$. For each ith subject, we compute the residual $\mathbf{e}_i$ of reconstructing $\mathbf{y}$ solely using the SPs coming from the ith subjects gallery series, say

$$\mathbf{e}_i = \mathbf{y} - \boldsymbol{\beta}^*\mathbf{X}_{(i)}. \tag{8}$$

As demonstrated by Wright *et al.* [47] in their work on sparse representation classification, the magnitude of $\mathbf{e}_i$

[2]Without introducing ambiguity, we denote an SP and its descriptor by the same symbol for notation convenience.

[3]Considering the gait pattern diversity and complexity when a large number of subjects exist, more homogenous groups need to be generated in practice than what we illustrated in Fig. 2.

suggests how dissimilar a sample $\mathbf{y}$ is to the known samples of the ith subject. In view of this, we use the ℓ^1-norm of the residual $\mathbf{e}_i$ to define the posterior probability of l given $\mathbf{y}$ in a softmax manner as

$$p(l=i|\mathbf{y}) = \frac{\exp(-\theta\|\mathbf{e}_i\|_1)}{\sum_{j=1}^{q}\exp(-\theta\|\mathbf{e}_j\|_1)} \tag{9}$$

where θ is a constant coefficient.[4]

Now, for the ith subject, let us write

$$\phi_i = \sum_{\mathbf{y}\in\mathcal{Y}} \ln p(l=i|\mathbf{y}). \tag{10}$$

Since l should normally follow a uniform distribution over $\{1, 2, \ldots, q\}$, say $p(l=i) = 1/q$, we obtain that

$$p(l=i|\mathcal{Y}) = \frac{\exp(\phi_i)}{\sum_{i=1}^{p}\exp(\phi_i)}. \tag{11}$$

With $p(l=i|\mathcal{Y})$ obtained, we realize identification by MAP, and realize verification by thresholding. In particular to verification, we take the first subject as the target, and the rest $(q-1)$ as the cohorts, which do not appear as impostors. Then, only $p(l=1|\mathcal{Y})$ is used as the verification score. The above classifier works for sparse code collections, like our SP-based representation of gait acceleration series, and is termed CSCC.

At last, we extend our algorithm for the multiaccelerometer case. When gait acceleration series are present for multiple body locations, we encode the SPs and estimate ls posterior with respect to a single SP [from Section III to (9)] independently for each series so that SPs from different series do not interfere with each other. After that, we put the SPs from all the series together as $\mathcal{Y}$, and compute $p(l=i|\mathcal{Y})$ using (10) and (11).

V. ZJU-GaitAcc Dataset

To support the research of accelerometer-based gait recognition, we built the ZJU-GaitAcc dataset and published it for open access.

As it was shown in Fig. 3, we measured gait acceleration by the Wii remotes[5] fastened at five body locations: 1) the left upper arm; 2) the right wrist; 3) the right side of the pelvis; 4) the left thigh; and 5) the right ankle. These locations covers the most important articulation structures of the human body. Considering the symmetry of the human gait, we left the mirrored body locations without sensors. The choice of the left or right side is randomly determined and fixed. It should not affect the discriminativeness of gait acceleration significantly.[6]

The Wii remote has an ADXL330 triaxial accelerometer, which can measures acceleration at least up to ± 3 g and typically to ± 5 g, where "g" denotes the gravitational constant.

[4]According to our experience, the value of θ has little influence on the recognition performance provided that the computational precision is sufficient for (11). However, in practice, θ has to be valued properly to avoid numerical underflow, which does affect the algorithm correctness.

[5]The Wii remote is the primary controller for Nintendo's Wii console.

[6]The symmetry of human gait is not strict, so equipping sensors on both side may result in a bit better discriminativeness than on a single side. However, wearing too many sensors may be a burden for the users. As a trade-off, we only used one side.

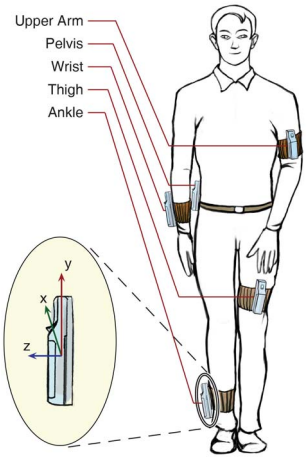

Fig. 3. Body locations wearing accelerometers.

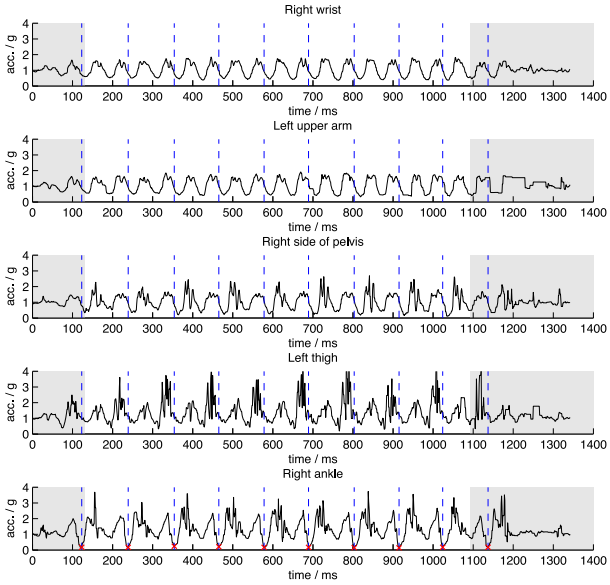

Fig. 4. Data illustration of ZJU-GaitAcc—gait acceleration series simultaneously obtained at five body locations. The highlighted segments are annotated to be useful. The blue dashed are the annotated cycle borders, which are located at the cyclic valley points marked by the red crosses in the subfigure for the right ankle.

The acceleration readings were measured with the precision of about (5/128)g and sent out in real time via bluetooth at frequencies up to 100 Hz. We used a laptop to receive the acceleration readings, and resampled them at exactly 100 Hz.

We asked the participants to naturally and straightly walk through a level floor of 20 m length. The recording began before they started to walk and ended after they stopped. Nonetheless, only the middle segments that corresponds to the walking periods are taken to be useful. We manually annotated the starting and ending points of the useful segments, where the badly collected cycles caused by unstable wireless communication at the two ends were eliminated in the meanwhile. Normally, the useful length of a record are 7–15 s.

To facilitate the research on gait analysis relying on cycle detection, we provided the manual annotations of the step cycles with ZJU-GaitAcc. As it was shown in Fig. 4, we manually

TABLE II
SUMMARY OF ZJU-GAITACC

Property	Value
# Subjects	175
# Recording sessions	2
# Subjects in both sessions (Session 1 & 2)	153
# Subjects in only one session (Session 0)	22
# Records per subject in one session	6
Time intervals between the two sessions	1wk~0.5yr
Floor length	$\approx$ 20m
Effective length of a record	[a]$\approx$ 7~15s
Effective full step cycles in a record	[a]$\approx$ 7~14
Sample frequency	100Hz

a. for 95% of all the records in ZJU-GaitAcc.

annotated[7] the cycle borders at the cyclic valley points of the gait acceleration series recorded at the ankle.[8] Normally, 7–14 full step cycles (one left and one right step constitute a full step) existed within the useful segment of a record.

To make ZJU-GaitAcc close to practical scenarios, we gave few instructions on the dress of the participants. They might wear any kind of clothes and shoes except the slippers, which are proven to have too strong impact on human gait patterns [48]. A participant might also dress in different ways for the two sessions. What is more, as we did not use particularly designed clothes or shoes for acceleration acquisition (they are used in some existing pieces of works, see [7]), the Wii remotes could not be mounted on the specific body locations very precisely for different participants and sessions. It imitated the practical scenarios of wearable and portable devices.

There were 175 volunteers participating in our data acquisition. One hundred and fifty-three of them were present in two sessions (Sessions 1 and 2) separated by one week to 0.5 year for different subjects so that the natural gait changes over time were incorporated into the dataset. The other 22 volunteers participated in only one session. To distinguish them from those appearing in both the two sessions, we grouped their records into a separate session, termed Session 0. For a single participate, six records were acquired in one session. Accordingly, we organized the records in each session into six batches.

The scale of ZJU-GaitAcc was large compared with existing datasets attached to previous work. One exception was Trung *et al.*'s dataset [34], which contains 736 subjects. Nevertheless, it had not been publicly accessible, and contained only the gait acceleration measured at one body location.

Based on the above specification, which were summarized in Table II, ZJU-GaitAcc turned out be challenging due to the following.

1) The natural gait changes over time.
2) The gait variations attributed to dress changes.
3) The variations of the accelerometer location and orientation.

[7]To reduce the cost of manual labeling, we in fact develop a semi-automatic algorithm to help us predetect the valley points. This algorithm can detect most (>95%) valley points with a small amount of human interaction. After that, we check all the series and correct the wrong and missing detections manually.

[8]We only annotated step cycles for the ankle, and applied them to all the other locations, at which it is more difficult to annotate step cycles.

ZJU-GaitAcc is open to public access at http://www.cs.zju.edu.cn/~gpan/database/gaitacc.html

Because of our agreement with the volunteers, we cannot release personal information, such as age and gender, with the dataset. However, a rough statistics can be found on the webpage.

VI. EXPERIMENTS

With the ZJU-GaitAcc dataset, we experimentally evaluated the proposed method in several aspects. First, we benchmarked it for all the possible combinations of the five body locations available in the dataset. Second, we inspected the internal procedure of our sparse coding scheme, and illustrated its effectiveness. Finally, we compared our algorithm with a few typical existing methods, where we considered both the performance in the common scenario and the robustness to the length limitation of gait acceleration series.

For identification, we took each batch of records in either Sessions 1 or 2 as the gallery and all the six batches in the other session as the probes. Session 0 was always merged into the gallery session. Thus, 6×2 sub-evaluations with 153 test cases are present, leading to 1836 test cases in total.

For verification, we partitioned the subjects in Sessions 1 and 2 into threefolds, and enumerately take each fold as the cohorts and the rest two as the testing set. For each iteration, every series in the testing set was taken as the known target once. Together with the cohort series in the same batch and same session, it formed the gallery (51 subjects). All the series in the other session of the target were taken as the probes. Unlike what we did for identification, Session 0 was always merged into the probe session, serving as impostors. The total number of the test cases is $\underbrace{3}_{\#\text{folds}} \times \underbrace{\left(153 \times \frac{2}{3} \times 6 \times 2\right)}_{\#\text{targets for fold}} \times \underbrace{\left((153 \times \frac{2}{3} + 22) \times 6\right)}_{\#\text{probes per target}} = 2\,731\,968$.[9] Note that for both identification and verification, only one series per subject existed in the gallery.

The parameters for our algorithm were set to the values shown in the following table.

Param.	h	σ_0	σ_{N}	γ	r_{id}	r_{vr}	u	v	θ
Value	21	1.2	0.2	2	200	100	1	8	50

Note that h is the dimension of the SP descriptor, σ_0 is the base scale, σ_N is the scale for the natural blur of the series, and γ is the scale factor (Section III-A). Since the multiscale SP is an extension of the single-scale SP used in [21], the values of h, σ_0, σ_N are chosen in consistent with the optimal parameters in [21]. Because the gallery sizes were different for identification and verification, the cluster number r was valued differently: $r = r_{\mathrm{id}}$ for identification and $r = r_{\mathrm{vr}}$ for verification. u is the number of chosen clusters and v is the maximum

[9]This protocol is very exhausting, as it covers all the possible testing pairs. For the sake of efficiency, a more commonly used protocol is to sample only a relatively small number (e.g., several thousands) of pairs for testing. Here, we value the reliability of the results more than the efficiency of the experiments, and use the most exhausting protocol.

TABLE III
IDENTIFICATION RATES OF VARIOUS BODY LOCATIONS

N.	Locations	RR (%)	EER (%)	N.	Locations	RR (%)	EER (%)
1	Wr	56.4	13.0	3	Wr, Up, Pv	86.0	5.2
	Up	63.9	9.9		Wr, Up, Th	87.1	4.4
	Pv	**73.4**	8.9		Wr, Up, Ak	87.2	4.2
	Th	68.3	**8.6**		Wr, Pv, Th	90.2	3.5
	Ak	68.8	9.5		Wr, Pv, Ak	91.8	3.2
2	Wr, Up	72.5	7.9		Wr, Th, Ak	90.9	3.1
	Wr, Pv	82.0	6.1		Up, Pv, Th	89.8	3.8
	Wr, Th	81.4	5.6		Up, Pv, Ak	91.4	3.3
	Wr, Ak	80.6	6.1		Up, Th, Ak	91.3	3.1
	Up, Pv	81.9	6.4		Pv, Th, Ak	**93.1**	**2.7**
	Up, Th	82.6	5.3	4	Wr, Up, Pv, Th	92.0	3.4
	Up, Ak	82.3	5.2		Wr, Pv, Th, Ak	93.3	2.9
	Pv, Th	85.6	4.4		Wr, Up, Th, Ak	93.7	2.7
	Pv, Ak	**87.5**	**4.1**		Wr, Up, Pv, Ak	**95.0**	**2.3**
	Th, Ak	86.1	4.2		Up, Pv, Th, Ak	94.9	2.4
5	Wr, Up, Pv, Th, Ak (All the 5 body locations)					**95.8**	**2.2**

Remark: Wr – (right) wrist; Up – (left) upper arm;
Pv – (right side of) pelvis; Th – (left) thigh; Ak – (right) ankle.

number of the nonzero entries (Section IV-A). Their values are chosen by cross-validation. θ is the constant multiplier in the softmax probability (Section IV-B).

In addition, our implementation is in MATLAB. When all the five available body locations were used, a single test case averagely took about 12 s for identification and 1.5 s[10] for verification on a desktop with a 4-core 3.07 GHz CPU and a 133 MHz frontal bus.[11] While such efficiency was already enough for practical usage, it would be improved by implementing the method in a less redundant language like C/C++. Our code can be downloaded at http://www.ytzhang.net/software/gait-sp/

A. Recognition With Different Combinations of Body Locations

Table III reported the performance of the proposed algorithm for all the possible combinations of the five body locations. Both the recognition rates (RRs, or the rank-1 accuracy) for identification and equal error rates (EERs) for verification were present.

The performance of algorithm gradually increased as more and more body locations were combined. The RRs for the combinations of 1–4 body locations were around 65%, 80%, 90%, and 93%, respectively; and, the EERs were around 11%, 6%, 4%, and 3%. By using all the five body locations, our algorithm achieved the RR of 95.8% and the EER of 2.2%. The increasing performance indicated that gait acceleration at distinct body locations contain mutually complementary information for profiling human gait in full scale. Our algorithm combined the discriminativeness of each body location for reliable recognition.

When a single body location was used, our algorithm performed the best at the pelvis for identification and at the thigh for verification. When 2–4 body locations were together used, the combinations of "pelvis + ankle," "pelvis + thigh + ankle," and "wrist + upper-arm + thigh + ankle," respectively achieved the best performance. According to Table III, the gait acceleration series recorded at the five different body locations generally made comparable contribution to the performance of our algorithm, while those at the pelvis, the thigh, and the ankle were more useful than those at the wrist and the upper arm. After all, the torso and legs are more responsible for human gait than the arms, as the arm motion is mainly for keep balance and can be varied without significant influence on the normal walk of people.

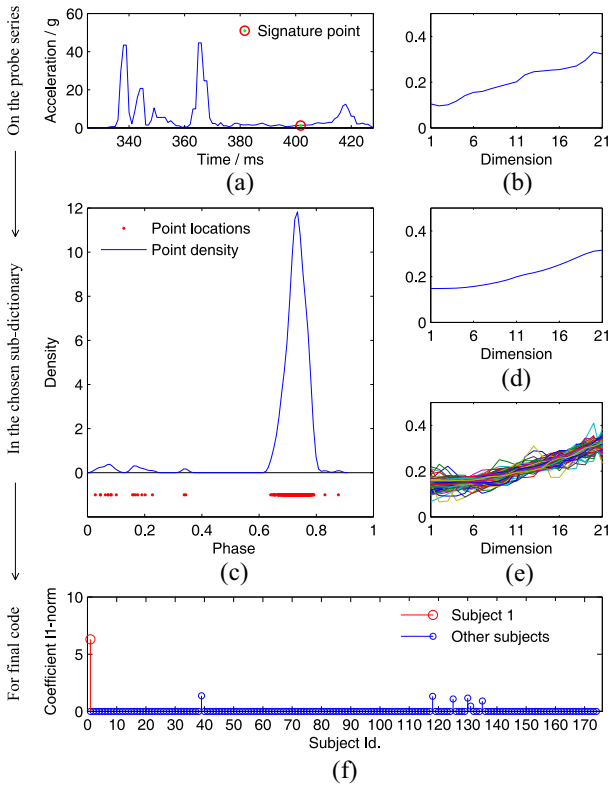

Fig. 5. Illustration of coding an SP from the acceleration series recorded at the right ankle. (a) SP on a probe series of Subject 1. (b) Its descriptor. (c) Phase distribution of the SPs in the selected sub-dictionary (composed of one cluster), whose summit is close to the phase of the given SP. (d) Center (mean) of the sub-dictionary, which is similar to the descriptor of the given SP. (e) All the elements of the sub-dictionary. (f) Coefficient distribution of the final code.

B. Effectiveness of the Sparse Coding Scheme for SPs

We illustrated the internal procedures of our sparse coding scheme for SPs using the identification settings.

Fig. 5 illustrated how an SP on a probe series is encoded. From the dictionary, which contains all the SPs from the gallery series, we took the cluster whose center [Fig. 5(d)] was most similar to the given SP [Fig. 5(b)] in terms of the descriptor as the chosen sub-dictionary. It turned out that the

[10]The reader may have noticed that, though the time consumption for a single test case is practical, the total time cost for performing the verification experiments might turn out to be huge (i.e., 50 days). Nevertheless, by running four parallel jobs on five machines, it can be done within three days.

[11]The time cost per test case was much less for verification than for identification. The causes were in twofolds: 1) the gallery set was smaller for verification and 2) as the test case number was much larger for verification, algorithm initialization, like clustering SPs, attributed to significantly less portion of the total time cost.

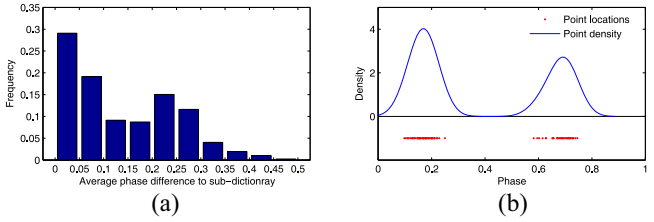

Fig. 6. Phase propinquity achieved by sub-dictionary selection. (a) We averaged the phase distances from an SP to the elements of its sub-dictionary, and showed the average-distance distribution of the SPs from all the probes. (b) Some SP clusters of the gallery series had two peaks in phase, which caused the high frequency between 0.2 and 0.3 in the first subfigure.

SPs in the sub-dictionary were also close to the given SP in terms of the step-cycle phase [Fig. 5(a) and (c)], which was consistent with our motivation for ensuring the phase propinquity in SP encoding. Then, we encoded the given SP with the chosen sub-dictionary [Fig. 5(e)]. The obtained coefficients concentrated in the groundtruth subject [Fig. 5(f)].

To further justify how effective the sub-dictionary selection is in realizing phase propinquity, we inspected the average phase distance[12] between a given SP and the elements of its corresponding sub-dictionary. Its distribution over the entire dataset was shown in Fig. 6(a). The frequency mostly concentrated in the interval of $[0, 0.1)$, and dropped rapidly as the distance increased, which indicated that most SPs were close to their corresponding sub-dictionaries in terms of the step-cycle phase. Admittedly, an exception happened in the interval of $[0.2, 0.3)$ due to the existence of clusters with double phase peaks, as it is shown in Fig. 6(b). Nevertheless, even in this case, half of the sub-dictionary elements were close to given SPs in terms of phase.

C. Comparison With Other Methods

We compared the proposed algorithm with four existing methods: 1) cycle matching [29]; 2) average cycle [27]; 3) eigenstep [28]; and 4) SP voting [21]. All the method were applied to the series of acceleration magnitude rather than other acceleration features. For cycle matching, average cycle, and eigenstep, we took the Euclidean distance as the similarity measurement. We also used the sum rule to fuse the scores obtained at multiple body locations so that these methods could work in the multiaccelerometer cases. For SP voting, we, on the one hand, conducted the original method, which uses the single-scale SP representation; on the other hand, we adapted it to the multiscale SP representation so as to demonstrate the effectiveness of the proposed extension on SP extraction. The latter setting was not actually an existing work, and was referred to as "msSP voting." While all the other mentioned methods can do both identification and verification, the SP and msSP voting can only do identification. The nontrivialness of being adapted to verification task is an important disadvantage of the SP and msSP voting compared with the proposed method.

All the above methods except ours require cycle detection. We directly used the step-cycle annotations provided in the dataset so that no cycle detection failures would happen and these methods would achieve the best possible performance, which is a kind of "cheating." We would show that the proposed method could perform the best, even when the other methods are cheating.

[12]For two SPs at phase $\beta_1, \beta_2 \in [0, 1)$, the phase distance of them is $\min(|\beta_2 - \beta_1|, 1 - |\beta_2 - \beta_1|) \in [0, 0.5]$.

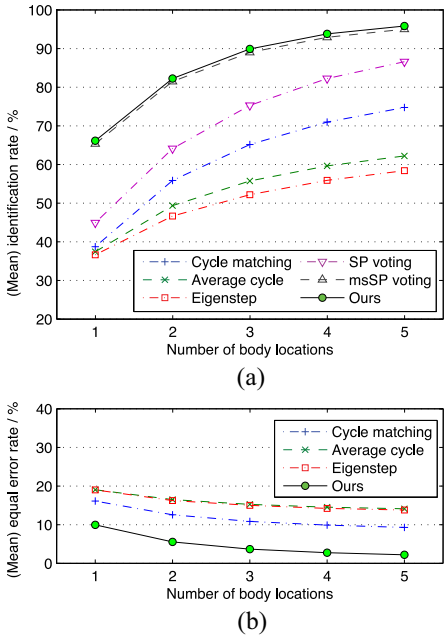

Fig. 7. Curves of average performance versus body location number for different methods. (a) (Mean) identification rates (RRs). (b) (Mean) EERs.

Moreover, the way that our algorithm uses the cohorts for verification [(11) in Section IV-B] may be considered as a type of score normalization, which can usually improves the performance of many methods. For the sake of fairness, we also normalized the scores in the other methods with the score summation on the gallery. Only the performance achieved with the normalized scores was reported, as it was always better than that with the unnormalized ones.

1) On Full Series: Fig. 7 reported the mean RRs and EERs with respect to the number of body locations. msSP voting outperformed the existing methods in our evaluations including SP voting, which gives evidence for the effectiveness of our multiscale extension for SP extraction. Our algorithm performed a little better than msSP voting for identification, and significantly better than the other methods for both identification and verification. Considering its independence on cycle detection, the superiority of our algorithm was noticeable. Overall, the performance of the methods are in the order: the proposed method $>$ msSP voting (identification only) $>$ SP voting (identification only) $>$ cycle matching $>$ average cycle $\approx$ eigenstep.[13]

We also reported their cumulative match characteristics (CMC) in Fig. 8 and receiver operating characteristics (ROC) in Fig. 9, where the best performing combinations for one, three, and five body locations were taken for illustration. In particular, the rank-5 accuracy of our algorithm

[13]Eigenstep was expected to perform significant better than average cycle [28]. However, methods based on PCA are generally sensitive to misalignment. Probably, the widely existing intercycle misalignment in ZJU-GaitAcc significantly harmed the performance of eigenstep.

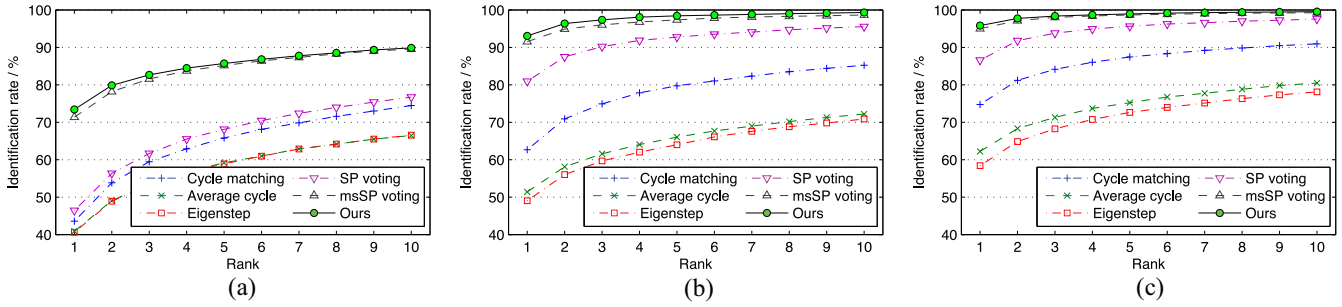

Fig. 8. CMC curves for different methods with various body locations. (a) Pelvis. (b) Pelvis, thigh, and ankle. (c) Wrist, upper arm, pelvis, thigh, and ankle.

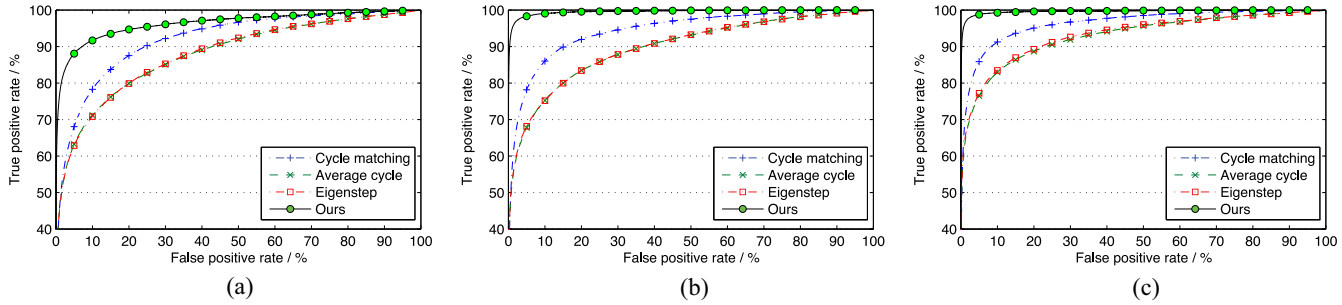

Fig. 9. ROC for different methods with various body locations. (a) Pelvis. (b) Pelvis, thigh, and ankle. (c) Wrist, upper arm, pelvis, thigh, and ankle.

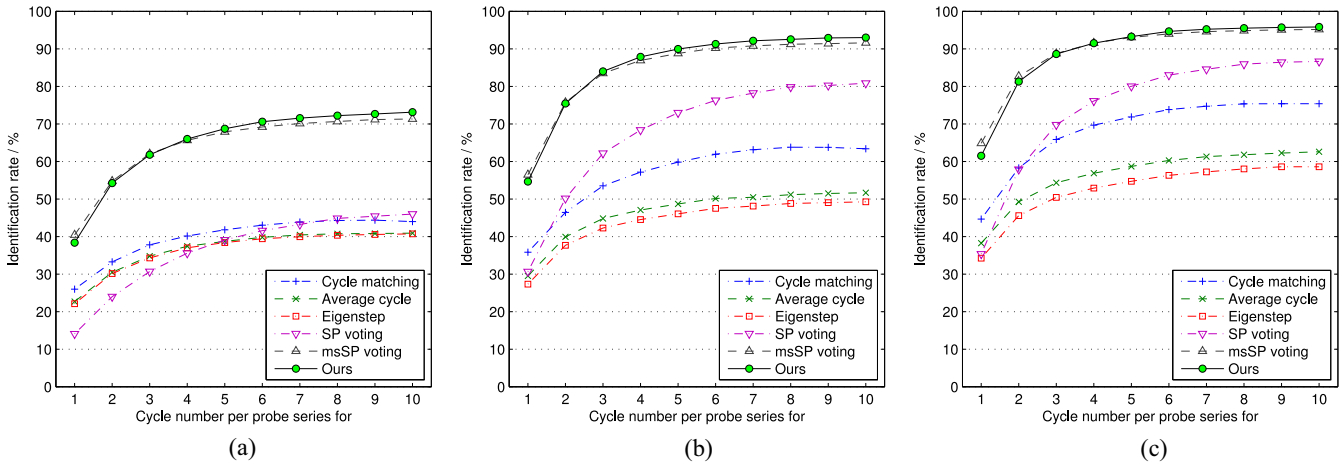

Fig. 10. Curves of identification rate versus probe cycle number for different methods. (a) Pelvis. (b) Pelvis, thigh, and ankle. (c) Wrist, upper arm, pelvis, thigh, and ankle.

for identification was nearly 99% when three and five body locations are used. The performance gap between other methods and ours became more noticeable on the ROC curves.

2) On Series of Controlled Lengths: In some practical scenarios, acquiring a long gait acceleration series without break might be difficult, so the algorithm performance on series with limited length is important. We evaluated identification with the probe series of different lengths. In particular, we took the sub-series consisting of the first given number of step cycles out of every probe series as the new probe series.

Fig. 10 reported the RRs for three body location combination cases. Though the SP-based methods appeared more sensitive to insufficient series lengths, our algorithm and msSP voting surpassed the others significantly even when only one step cycle was used. When five step cycles were present in a probe series, our algorithm could already achieve fairly good performance.

An additional experiment was performed in order to demonstrate the effectiveness of CSCC in fusing the weak classification results on individual SPs into a reliable one. In this experiment, only one SP is used for predicting the identity of a series. We did this for each SP, and the RR in this case was only 10.5%. Comparing it with the performance of our algorithm on entire probe series, we can notice the importance of the probabilistic fusing in CSCC.

VII. Conclusion

In this paper, we propose an accelerometer-based gait recognition method, which consists of a multiscale SP extraction method, an SP sparse encoding scheme with implicit

considering the phase propinquity, and the CSCC framework for recognizing feature collection. Our method avoids the two problems that many existing methods suffers from, i.e., cycle detection failures and intercycle phase misalignment. Its efficacy is demonstrated by experimental results on the ZJU-GaitAcc dataset.

REFERENCES

[1] G. Pan *et al.*, "Trace analysis and mining for smart cities: Issues, methods, and applications," *IEEE Commun. Mag.*, vol. 51, no. 6, pp. 120–126, Jun. 2013.

[2] Z. Wu and G. Pan, *SmartShadow: Models and Methods for Pervasive Computing*. Berlin, Germany: Springer, 2013.

[3] K. Liu *et al.*, "Measuring physical activity in peripheral arterial disease: A comparison of two physical activity questionnaires with an accelerometer," *Angiology*, vol. 51, no. 2, pp. 91–100, 2000.

[4] L. Bao and S. Intille, "Activity recognition from user-annotated acceleration data," in *Pervasive Computing* (Lecture Notes in Computer Science), vol. 3001, A. Ferscha and F. Mattern, Eds. Berlin, Germany: Springer, 2004, pp. 1–17.

[5] N. Ravi, N. Dandekar, P. Mysore, and M. L. Littman, "Activity recognition from accelerometer data," in *Proc. 17th Conf. Innov. Appl. Artif. Intell. (IAAI)*, vol. 3. 2005, pp. 1541–1546.

[6] G. Pan *et al.*, "GeeAir: A universal multimodal remote control device for home appliances," *Pers. Ubiquit. Comput.*, vol. 14, no. 8, pp. 723–735, Dec. 2010.

[7] D. Gafurov, P. Bours, and E. Snekkenes, "User authentication based on foot motion," *Signal Image Video Process.*, vol. 5, no. 4, pp. 457–467, 2011.

[8] K. Tong and M. Granat, "A practical gait analysis system using gyroscopes," *Med. Eng. Phys.*, vol. 21, no. 2, pp. 87–94, 1999.

[9] K. Aminian, B. Najafi, C. Büla, P. Leyvraz, and P. Robert, "Spatio-temporal parameters of gait measured by an ambulatory system using miniature gyroscopes," *J. Biomech.*, vol. 35, no. 5, pp. 689–699, 2002.

[10] R. Soames, "Foot pressure patterns during gait," *J. Biomed. Eng.*, vol. 7, no. 2, pp. 120–126, 1985.

[11] K. Koho, J. Suutala, T. Seppänen, and J. Röning, "Footstep pattern matching from pressure signals using segmental semi-Markov models," in *Proc. Eur. Signal Process. Conf. (EUSIPCO)*, 2004, pp. 1609–1612.

[12] Y. Shoji, A. Itai, and H. Yasukawa, "Personal identification using footstep detection in in-door environment," *IEICE Trans. Fundam. Electron. Commun. Comput. Sci.*, vol. E88-A, pp. 2072–2077, Aug. 2005.

[13] S. Niyogi and E. Adelson, "Analyzing and recognizing walking figures in XYT," in *Proc. IEEE Comput. Soc. Conf. Comput. Vis. Pattern Recognit. (CVPR)*, Seattle, WA, USA, 1994, pp. 469–474.

[14] P. Huang, "Automatic gait recognition via statistical approaches for extended template features," *IEEE Trans. Syst., Man, Cybern. B, Cybern.*, vol. 31, no. 5, pp. 818–824, Oct. 2001.

[15] L. Lee and W. E. L. Grimson, "Gait analysis for recognition and classification," in *Proc. 5th IEEE Int. Conf. Autom. Face Gesture Recognit. (FG)*, Washington, DC, USA, 2002, pp. 148–155.

[16] L. Wang, T. Tan, H. Ning, and W. Hu, "Silhouette analysis-based gait recognition for human identification," *Pattern Anal. Mach. Intell.*, vol. 25, no. 12, pp. 1505–1518, 2003.

[17] J. Zhang, J. Pu, C. Chen, and R. Fleischer, "Low-resolution gait recognition," *IEEE Trans. Syst., Man, Cybern. B, Cybern.*, vol. 40, no. 4, pp. 986–996, Aug. 2010.

[18] M. Goffredo, I. Bouchrika, J. Carter, and M. Nixon, "Self-calibrating view-invariant gait biometrics," *IEEE Trans. Syst., Man, Cybern. B, Cybern.*, vol. 40, no. 4, pp. 997–1008, Aug. 2010.

[19] R. Liu, Z. Duan, J. Zhou, and M. Liu, "Identification of individual walking patterns using gait acceleration," in *Proc. 1st Int. Conf. Bioinformat. Biomed. Eng. (ICBBE)*, 2007, pp. 543–546.

[20] M. Derawi, C. Nickel, P. Bours, and C. Busch, "Unobtrusive user-authentication on mobile phones using biometric gait recognition," in *Proc. 6th Int. Conf. Intell. Inf. Hiding Multimedia Signal Process. (IIH-MSP)*, 2010, pp. 306–311.

[21] G. Pan, Y. Zhang, and Z. Wu, "Accelerometer-based gait recognition via voting by signature points," *Electron. Lett.*, vol. 45, no. 22, pp. 1116–1118, Oct. 2009.

[22] J. Mäntyjärvi *et al.*, "Identifying users of portable devices from gait pattern with accelerometers," in *Proc. IEEE Int. Conf. Acoust. Speech Signal Process. (ICASSP)*, 2005, pp. 973–976.

[23] H. J. Ailisto, M. Lindholm, J. Mäntyjärvi, E. Vildjiounaite, and S.-M. Makela, "Identifying people from gait pattern with accelerometers," *Proc. SPIE*, vol. 5779, pp. 7–14, Apr. 2005.

[24] D. Gafurov, K. Helkala, and T. Søndrol, "Gait recognition using acceleration from MEMS," in *Proc. 1st Int. Conf. Avail. Rel. Security (ARES)*, 2006.

[25] D. Gafurov, K. Helkala, and T. Søndrol, "Biometric gait authentication using accelerometer sensor," *J. Comput.*, vol. 1, no. 7, pp. 51–59, 2006.

[26] E. Vildjiounaite *et al.*, "Unobtrusive multimodal biometrics for ensuring privacy and information security with personal devices," in *Pervasive Computing* (Lecture Notes in Computer Science), vol. 3968. Berlin, Germany: Springer, 2006, pp. 187–201.

[27] D. Gafurov, E. Snekkenes, and P. Bours, "Gait authentication and identification using wearable accelerometer sensor," in *Proc. IEEE Workshop Autom. Identif. Adv. Technol.*, Alghero, Italy, Jul./Aug. 2007, pp. 220–225.

[28] P. Bours and R. Shrestha, "Eigensteps: A giant leap for gait recognition," in *Proc. 2nd Int. Workshop Security Commun. Netw. (IWSCN)*, 2010, pp. 1–6.

[29] D. Gafurov, E. Snekkenes, and P. Bours, "Improved gait recognition performance using cycle matching," in *Proc. IEEE 24th Int. Conf. Adv. Inf. Netw. Appl. Workshops (WAINA)*, Perth, WA, USA, Apr. 2010, pp. 836–841.

[30] F. Juefei-Xu, C. Bhagavatula, A. Jaech, U. Prasad, and M. Savvides, "Gait-ID on the move: Pace independent human identification using cell phone accelerometer dynamics," in *Proc. IEEE 5th Int. Conf. Biometrics Theory Appl. Syst. (BTAS)*, 2012, pp. 8–15.

[31] R. Liu, J. Zhou, M. Liu, and X. Hou, "A wearable acceleration sensor system for gait recognition," in *Proc. 2nd IEEE Conf. Ind. Electron. Appl. (ICIEA)*, Harbin, China, 2007, pp. 2654–2659.

[32] M. Derawi, P. Bours, and K. Holien, "Improved cycle detection for accelerometer based gait authentication," in *Proc. 6th Int. Conf. Intell. Inf. Hiding Multimedia Signal Process. (IIH-MSP)*, Darmstadt, Germany, 2010, pp. 312–317.

[33] N. T. Trung *et al.*, "Phase registration in a gallery improving gait authentication," in *Proc. Int. Joint Conf. Biometrics (IJCB)*, Washington, DC, USA, 2011, pp. 1–7.

[34] N. T. Trung, Y. Makihara, H. Nagahara, Y. Mukaigawa, and Y. Yagi, "Performance evaluation of gait recognition using the largest inertial sensor-based gait database," in *Proc. 5th IAPR Int. Conf. Biometrics (ICB)*, New Delhi, India, 2012, pp. 360–366.

[35] C. Nickel, C. Busch, S. Rangarajan, and M. Mobius, "Using hidden Markov models for accelerometer-based biometric gait recognition," in *Proc. 7th IEEE Int. Colloq. Signal Process. Appl. (CSPA)*, Penang, Malaysia, 2011, pp. 58–63.

[36] S. J. Morris, "A shoe-integrated sensor system for wireless gait analysis and real-time therapeutic feedback," Ph.D. dissertation, Harvard/MIT Div. Health Sci. Technol., Cambridge, MA, USA, 2004.

[37] D. Gafurov, E. Snekkenes, and T. Buvarp, "Robustness of biometric gait authentication against impersonation attack," in *Proc. OTM Workshops Move Meaningful Internet Syst.*, 2006, pp. 479–488.

[38] D. Gafurov, E. Snekkenes, and P. Bours, "Spoof attacks on gait authentication system," *IEEE Trans. Inf. Forensics Security*, vol. 2, no. 3, pp. 491–502, Sep. 2007.

[39] M. Turk and A. Pentland, "Eigenfaces for recognition," *J. Cogn. Neurosci.*, vol. 3, no. 1, pp. 71–86, 1991.

[40] Y. Makihara *et al.*, "Phase registration of a single quasi-periodic signal using self dynamic time warping," in *Proc. 10th Asian Conf. Comput. Vis. (ACCV)*, vol. 3. 2011, pp. 667–678.

[41] M. McGuire, "An overview of gait analysis and step detection in mobile computing devices," in *Proc. 4th Int. Conf. Intell. Netw. Collab. Syst. (INCoS)*, 2012, pp. 648–651.

[42] D. Lowe, "Distinctive image features from scale-invariant keypoints," *Int. J. Comput. Vis.*, vol. 60, no. 2, pp. 91–110, 2004.

[43] J. Perry, *Gait Analysis: Normal and Pathological Function*. Thorofare, NJ, USA: SLACK, 1992, pp. 9–16.

[44] Y. Pati, R. Rezaiifar, and P. S. Krishnaprasad, "Orthogonal matching pursuit: Recursive function approximation with applications to wavelet decomposition," in *Proc. 27th Asilomar Conf. Signals Syst. Comput. (ACSSC)*, vol. 1. Pacific Grove, CA, USA, 1993, pp. 40–44.

[45] J. Tropp and A. Gilbert, "Signal recovery from random measurements via orthogonal matching pursuit," *IEEE Trans. Inf. Theory*, vol. 53, no. 12, pp. 4655–4666, Dec. 2007.

[46] M. Aharon, M. Elad, and A. Bruckstein, "*K*-SVD: An algorithm for designing overcomplete dictionaries for sparse representation," *IEEE Trans. Signal Process.*, vol. 54, no. 11, pp. 4311–4322, Nov. 2006.

[47] J. Wright, A. Yang, A. Ganesh, S. Sastry, and Y. Ma, "Robust face recognition via sparse representation," *IEEE Trans. Pattern Anal. Mach. Intell.*, vol. 31, no. 2, pp. 210–227, Feb. 2009.
[48] M. S. Nixon, T. Tan, and R. Chellappa, *Human Identification Based on Gait*, vol. 4. New York, NY, USA: Springer, 2006.

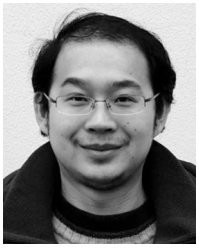

Yuting Zhang received the B.E. degree in computer science from Zhejiang University, Hangzhou, China, in 2009, where he is currently pursuing the Ph.D. degree from the Department of Computer Science, advised by G. Pan.

He was a Junior Research Assistant with the Advanced Digital Sciences Center, Singapore, and the University of Illinois at Urbana-Champaign, Urbana, IL, USA, in 2012. His current research interests include computer vision, pattern recognition, and biometric modalities.

Gang Pan received the B.Sc. and Ph.D. degrees in computer science from Zhejiang University, Hangzhou, China, in 1998 and 2004, respectively.

He is currently a Professor with the College of Computer Science and Technology, Zhejiang University. He was with the University of California, Los Angeles, Los Angeles, CA, USA, as a Visiting Scholar, from 2007 to 2008. His current research interests include pervasive computing, computer vision, and pattern recognition. He has co-authored over 100 refereed papers. He has also served as a Program Committee Member for over ten prestigious international conferences and as a Reviewer for various leading journals.

Kui Jia received the B.Eng. degree in marine engineering from the Northwestern Polytechnical University, Xi'an, China, the M.Eng. degree in electrical and computer engineering from the National University of Singapore, Singapore, and the Ph.D. degree in computer science from the Queen Mary University of London, London, U.K., in 2001, 2003, and 2007, respectively.

He is currently a Visiting Assistant Professor with the Faculty of Science and Technology, University of Macau, Macau, China. His current research interests include computer vision, machine learning, and image processing.

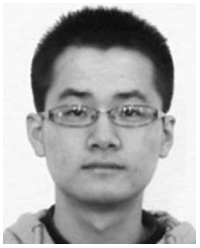

Minlong Lu received the B.E. degree in computer science from Zhejiang University, Hangzhou, China, in 2011, where he is currently pursuing the Ph.D. degree from the Department of Computer Science, advised by G. Pan.

His current research interests include computer vision and pattern recognition.

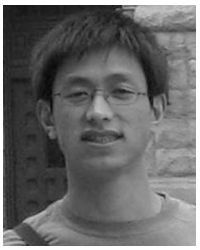

Yueming Wang received the Ph.D. degree from the Department of Computer Science and Technology, Zhejiang University, Hangzhou, China, in 2007.

From 2007 to 2010, he was a Post-Doctoral Fellow with the Department of Information Engineering, Chinese University of Hong Kong, Hong Kong. Since 2010, he has been an Associate Professor of computer science with the Qiushi Academy for Advanced Studies, Zhejiang University. His current research interests include computer vision, statistical pattern recognition, and brain–machine interface.

Zhaohui Wu received the Ph.D. degree in computer science from Zhejiang University, Hangzhou, China, in 1993. From 1991 to 1993, he was with the German Research Center for Artificial Intelligence as a joint Ph.D. student in the area of knowledge representation and expert system.

He is currently a Professor of Computer Science with Zhejiang University and the Director of the Institute of Computer System and Architecture, Zhejiang University, Hangzhou, China. He has authored five books and over 200 refereed papers. His current research interests include intelligent systems, semantic grid, and ubiquitous embedded systems. He is with the editorial boards of several journals and has served as a Program Committee member for various international conferences.